Plant Mol Biol (2011) 77:513–528
DOI 10.1007/s11103-011-9828-3

Mapping cell fate decisions that occur during soybean defense responses

Prachi D. Matsye · Ranjit Kumar · Parsa Hosseini · Christina M. Jones · Arianne Tremblay · Nadim W. Alkharouf · Benjamin F. Matthews · Vincent P. Klink

Received: 12 August 2011 / Accepted: 10 September 2011 / Published online: 11 October 2011

Abstract The soybean defense response to the soybean cyst nematode was used as a model to map at cellular resolution its genotype-defined cell fate decisions occurring during its resistant reactions. The defense responses occur at the site of infection, a nurse cell known as the syncytium. Two major genotype-defined defense responses exist, the *G. max*$_{[Peking]}$- and *G. max*$_{[PI\ 88788]}$-types. Resistance in *G. max*$_{[Peking]}$ is potent and rapid, accompanied by the formation of cell wall appositions (CWAs), structures known to perform important defense roles. In contrast, defense occurs by a potent but more prolonged reaction in *G. max*$_{[PI\ 88788]}$, lacking CWAs. Comparative transcriptomic analyses with confirmation by Illumina® deep sequencing were organized through a custom-developed application, Pathway Analysis and Integrated Coloring of Experiments (PAICE) that presents gene expression of these cytologically and developmentally distinct defense responses using the Kyoto Encyclopedia of Genes and Genomes (KEGG) framework. The analyses resulted in the generation of 1,643 PAICE pathways, allowing better understanding of gene activity across all chromosomes. Analyses of the *rhg1* resistance locus, defined within a 67 kb region of DNA demonstrate expression of an amino acid transporter and an α soluble NSF attachment protein gene specifically in syncytia undergoing their defense responses.

Keywords Soybean · *Glycine max* · Soybean cyst nematode · SCN · *Heterodera glycines* · Microarray · Gene expression · Plant pathogen · Parasite · Affymetrix® · Laser capture microdissection · PI 88788 · Peking · PI 548402 · Transcriptome, genome, gene expression, pathway analyses, *rhg1*, KEGG · Pathway Analysis and Integrated Coloring of Experiments · PAICE · Resistance · Illumina®

The authors Prachi D. Matsye, Ranjit Kumar contributed equally to the work.

Electronic supplementary material The online version of this article (doi:10.1007/s11103-011-9828-3) contains supplementary material, which is available to authorized users.

P. D. Matsye · C. M. Jones · V. P. Klink (✉)
Department of Biological Sciences, Mississippi State University, Mississippi State, MS 39762, USA
e-mail: vklink@biology.msstate.edu

R. Kumar
Center of Biostatistics and Bioinformatics, University of Mississippi Medical Center, Arthur C. Guyton Research Complex, G-651, 2500 North State Street, Jackson, MS 39216, USA

P. Hosseini · N. W. Alkharouf
Department of Computer and Information Sciences, Jess and Mildred Fisher College of Science and Mathematics, Towson University, Towson, MD 21252, USA

A. Tremblay · B. F. Matthews
Henry A. Wallace Beltsville Agricultural Research Center, Plant Sciences Institute, Soybean Genomics and Improvement Laboratory, United States Department of Agriculture-Agricultural Research Service, Bldg. 006, Beltsville, MD 20705, USA

Introduction

The dominant pathogen of *Glycine max* (L.) Merr. (soybean) is the parasitic nematode *Heterodera glycines* Ichinohe (soybean cyst nematode [SCN]), an invasive species first observed in the U.S. in 1954 (Winstead et al. 1955). The SCN reproduces on at least 97 legume and 63 non-legume hosts (Epps and Chambers 1958; Riggs and

Hamblen 1962, 1966a, b) with new hosts determined on a regular basis (Creech and Johnson 2006). SCN causes 7–10% reduction in production, worldwide. SCN causes more economic damage than the rest of its pathogens combined (Wrather and Koenning 2006), resulting in about $1.5 billion in losses in the U.S. alone, annually. Approximately 20,000 publically available collections of *G. max*, classified as plant introductions (PIs), are maintained through the USDA National Plant Germplasm System (USDA-NPGS). This seed bank, including many natural collections, is a resource that has been screened to identify *G. max* germplasm that can resist *H. glycines* infection. Through screening studies, two major groups of PIs each composed of a few *G. max* genotypes have been shown to exhibit specific, but contrasting ways to combat *H. glycines* (Ross and Brim 1957; Ross 1958; reviewed in Riggs 1992). Defense occurs at the site of infection, a nurse cell known as a syncytium (Fig. 1). The cellular response of *G. max*$_{[\text{Peking}]}$ to SCN has been determined (Ross 1958) and other genotypes including PI 89772, PI 90763 and partially PI 437654 (Mahalingham and Skorupska 1996) have been found to defend against SCN in a similar manner. The *G. max*$_{[\text{PI 88788}]}$ genotype was identified from a second screen (Epps and Hartwig 1972) with PI 209332, PI 548316 and partially PI 437654 (Mahalingham and Skorupska 1996) having similar cytological features occurring during their defense responses.

Numerous studies have investigated the soybean defense responses to SCN. The *G. max*$_{[\text{Peking}]}$ defense response is potent and rapid because most nematodes die early during parasitism at the parasitic second stage juvenile (p-J2) stage (Colgrove and Niblack 2008). The *G. max*$_{[\text{Peking}]}$-type of defense response is evident at the cellular level at 4 dpi, involves necrosis of the cells that surround the head of the nematode and separates the syncytium from the cells that surround it (Endo 1964, 1965; Riggs et al. 1973; Kim et al. 1987; Kim and Riggs 1992). Another defining feature of the *G. max*$_{[\text{Peking}]}$-type of defense response is the presence of cell wall appositions (CWAs), structures defined as physical and chemical barriers to cell penetration (Aist 1976, Schmelzer 2002; Hardham et al. 2008). In contrast, the *G. max*$_{[\text{PI 88788}]}$ defense response is potent but prolonged as the nematodes die at the J3 or J4 stages (Acido et al. 1984; Kim et al. 1987; Colgrove and Niblack 2008). In contrast to the *G. max*$_{[\text{Peking}]}$-type of defense, the *G. max*$_{[\text{PI 88788}]}$-type of response lacks the development of a necrotic layer that surrounds the head of the nematode (Kim et al. 1987). The initial stages of the *G. max*$_{[\text{PI 88788}]}$-type of defense response involves extensive accumulation of cisternae and rough ER that is accompanied by nuclear degeneration within the syncytium by 5 dpi (Kim et al. 1987). The *G. max*$_{[\text{PI 88788}]}$-type of defense response lacks thickened cell walls or appositions.

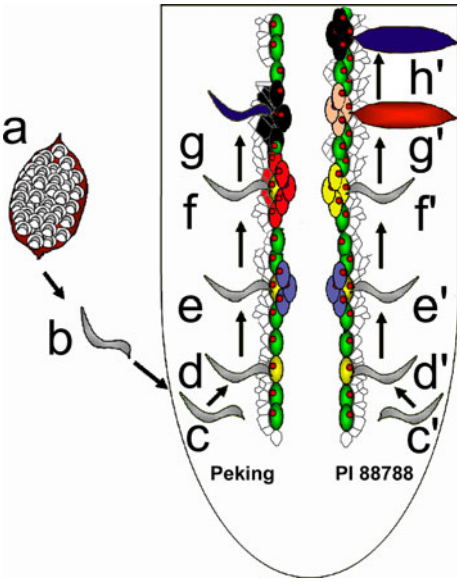

Fig. 1 *G. max*$_{[\text{Peking/PI 548402}]}$ and *G. max*$_{[\text{PI 88788}]}$ resistant reactions. The phase 1 period of the defense response is represented in *c*, *c′* through *e*, *e′*. The phase 2 period of the defense response is represented in *f*, *f′* through *h′*. *a* Cyst containing eggs. *b* Pre-infective J2 (pi-J2) nematodes (*gray*) migrate toward the root. *c*, *c′* the infective J2 (i-J2) nematodes burrow into the root and migrate toward the root stele, *d*, *d′*, the parasitic J2 (p-J2) typically selects a pericycle (*green cells*) or neighboring cell as the feeding site initial (FS_i) (*yellow cell*). This cell is used to initiate the formation of the syncytium. The earlier stages of syncytium development (between 1 and 4 dpi) are similar between *G. max*$_{[\text{Peking}]}$ and *G. max*$_{[\text{PI 88788}]}$-type of resistant reactions. *e′* In *G. max*$_{[\text{Peking}]}$-type, the neighboring cells (*purple*) are incorporated into the syncytium at 3 dpi. *e′* In *G. max*$_{[\text{PI 88788}]}$, the neighboring cells (*purple*) are incorporated into the syncytium at 3 dpi. *f* In *G. max*$_{[\text{Peking}]}$, a rapid and potent resistant reaction occurs by the formation of a necrotic region that surrounds the syncytium (*red layer* of cells surrounding the *yellow* FS_i) by 4 dpi. *f′* In *G. max*$_{[\text{PI 88788}]}$, a prolonged but potent resistant reaction at the syncytium (*pink cells*) is not yet evident at the cytological level at 4 dpi. *g* In *G. max*$_{[\text{Peking}]}$, degradation of the syncytium (*black cells*) is engaged that is accompanied by the mortality of the SCN at the p-j2 stage (*purple nematode*). *g′* In contrast, in *G. max*$_{[\text{PI 88788}]}$, the syncytium (*pink cells*) continues to develop until 5 dpi. The SCN feeding from the syncytium continues to develop, molting into J3s (*red nematode*). *h′* In *G. max*$_{[\text{PI 88788}]}$, the entire syncytium collapses (*black cells*) and the SCN dies at the J3 or J4 stage (*purple nematode*). (The timing of stages is adapted from Endo 1965; Riggs et al. 1973; Lauritis et al. 1983; Kim et al. 1987)

The genetic basis underlying defense to SCN resulted in the identification of the major recessive (*rhg1*, *rhg2* and *rhg3*) (Caldwell et al. 1960), and dominant (*Rhg4*) (Matson and Williams 1965) and *Rhg5* (Rao-Arelli 1994) loci. Of these, the *rhg1* locus is currently the best understood since it has been defined in a region spanning approximately 611,794 nucleotides on chromosome 18 (Concibido et al. 1994; Mudge et al. 1997; Cregan et al. 1999; Hyten et al. 2010). Allelic variants are known to exist between different soybean genotypes harboring *rhg1* (Brucker et al. 2005; Kim et al. 2010). Furthermore, fine mapping efforts in the

G. max$_{[PI\ 88788]}$ background has allowed the locus to be narrowed down to within a region of approximately 67 kb (Kim et al. 2010).

While mapping efforts have made large contributions to understanding resistance, recent evidence has shown the value in applying gene expression to compliment mapping efforts in plants with complex duplicated genomes (Bancroft et al. 2011). The availability of the *G. max* genome (Schmutz et al. 2010) allows for similar expression mapping to be performed. However, expression studies typically examine differentially expressed genes whereby expression is measured in both a control and experimental sample and relative levels of expression are compared under various statistical parameters. The problem with the differential expression approach is that genes that have expression in one sample type and lack expression in a second sample type are discarded because statistical analyses cannot be done when expression is lacking in one of the two samples (Fig. 2). Detection call methodology (DCM) makes possible the cross-comparison of gene activity measured in one sample type to a second sample type where activity is not measured. Therefore, it is possible to identify and analyze genes with expression that is limited to one cell type. The important concept to recognize is that this pool of expressed genes could represent gene activity that defines a specialized cell type such as a syncytium proceeding through a series developmental events that culminates in a terminal phenotype such as cell death. Therefore, it could be imagined that an undifferentiated cell type like pericycle would lack expression of genes involved in programmed cell death where they would be found to be expressed in a syncytium undergoing the terminal steps of resistance. Thus, DCM in concert with differential expression analyses could provide a broader and more comprehensive analysis of gene expression in specialized cell types such as syncytia undergoing defense.

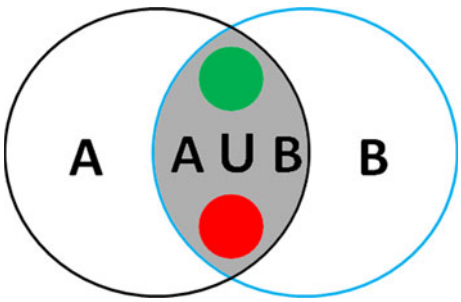

Fig. 2 Detection call methodology. *A* and *B* represent genes with measured detection from two different cell types. The *center gray region*, which represents the union of *A* and *B* having the same pool of genes, including the *green pool* (induced genes) and *red pool* (suppressed genes), are genes that can be analyzed by differential expression analyses because they are expressed in both sample types. The *gray region*, lacking the *red* and *green pools* are the genes expressed in both sample types but do not exhibit statistically significant differences in expression between *A* and *B*. The genes of the *white region* of the *A* pool do not meet the statistical criteria of differential expression studies and would be discarded because they are expressed in only one sample type. Likewise, the genes in the *white region* of pool *B* pool are those that are discarded in differential expression studies. The *white pools* of genes are the focus of the detection call methodology

The analysis presented here compares gene expression occurring during the potent and rapid defense response found in *G. max*$_{[Peking/PI\ 548402]}$ to the potent but prolonged process found in *G. max*$_{[PI\ 88788]}$. Expression is presented graphically using a custom-developed KEGG application called Pathway Analysis and Integrated Coloring of Experiments (PAICE) (Hosseini et al. unpublished). Comparative analyses of transcriptional activity in these cytologically and developmentally distinct defense responses are used to determine gene expression in relation to the sequenced genome of *G. max*$_{[Williams\ 82/PI\ 518671]}$, identifying the chromosomal coordinates of the expressed genes. Further analyses place the expressed genes in relationship to an important resistance locus, *rhg1*, defined within a 67 kb region of DNA on chromosome 18 between the markers BARCSOYSSR_18_0090 and BARCSOYSSR_18_0094 (Kim et al. 2010). Gene expression of a subset of 1,000 genes is confirmed by Illumina® deep sequencing.

Materials and methods

Plant and nematode procurement

The materials and methods pertaining to *H. glycines* populations, *G. max* genotypes, experimental procedures and data analysis methods are published (Klink et al. 2005, 2007, 2009; Alkharouf et al. 2006). The *G. max*$_{[Peking/PI\ 548402]}$ and *G. max*$_{[PI\ 88788]}$ stocks were originally obtained from the USDA-NPGS (http://www.ars-grin.gov/npgs/acc/acc_queries.html). The *H. glycines* NL1-RHg population used in the studies is race 3, HG-type 7 (*H. glycines*$_{[NL1\text{-}RHg/HG\text{-}type\ 7]}$) (Klink et al. 2009, 2010a). The *G. max*$_{[Peking/PI\ 548402]}$ and *G. max*$_{[PI\ 88788]}$ genotypes were used in the experiments to obtain defense responses by the use of *H. glycines*$_{[NL1\text{-}RHg/HG\text{-}type\ 7]}$. The *H. glycines*$_{[TN8/HG\text{-}type\ 1.3.6.7]}$ (race 14) population was used to obtain susceptible reactions (Klink et al. 2007, 2009, 2010a). Seedlings were grown according to Klink et al. (2007, 2009). Prior to infection, the nematodes were diluted to a final concentration of 2,000 pi-J2/ml and one ml of nematode stock was added to each root of each plant. The roots, including the mock-infected control samples, were washed after 1 day to remove nematodes that had not penetrated the roots. Infected roots were grown for 3, 6 or 9 dpi. Maximally infected lateral roots were harvested for analyses. The process was subsequently repeated twice, providing three independent sets of samples for each genotype.

LCM and microarray hybridization

Slides were prepared according to Klink et al. (2005, 2007, 2009, 2010a). LCM was performed on a Leica® ASLMD microscope® (Leica®). Serial sections of approximately 100 syncytia were used to obtain the RNA for the studies for each replicate. Over 100 ng of RNA per replicate was obtained for the studies. Work to obtain RNA was done with the PicoPure RNA Isolation kit, (Molecular Devices®). A DNAse treatment was added, just before the second column wash, using DNAfree® (Ambion®). RNA quality and yield were determined using the RNA 6000 Pico Assay® (Agilent Technologies®) using the Agilent 2100 Bioanalyzer® according to the manufacturer's instructions. Both probe preparation and hybridization procedures on the GeneChip® Soybean Genome Array (Affymetrix®) were performed according to their guidelines.

Data analysis

All microarray hybridizations were performed at the Laboratory of Molecular Technology, SAIC-Frederick, National Cancer Institute at Frederick, Frederick, MD 21701, USA. Local normalization was used. The measurement of the presence or absence of transcripts by particular probe set on a single array was determined using the Bioconductor implementation of the standard Affymetrix® DCM according to Klink et al. (2010b). In summary, the DCM consists of four steps: (1) removal of saturated probes, (2) calculation of discrimination scores, (3) *P*-value calculation using the Wilcoxon's rank test, and (4) the detection (present/marginal/absent). Ultimately, the algorithm determines if the presence of a probe set's transcript is provably different from zero (present [P]), uncertain (marginal [M]), or not provably different from zero (absent [A]). A probe set was considered present only if it measured expression on all three replicate microarrays corresponding to that condition. To be considered absent, the probe set had to lack detection on all three replicates for a given condition. A description of the supplemental files is provided. Microarray gene expression has been confirmed using the Illumina® Genome Analyzer II® (Illumina®) at the USDA-ARS Beltsville, MD according to the manufacturer's protocols. Data is maintained at the Soybean Genomics and Microarray Database (Alkharouf and Matthews 2004).

Gene pathway analyses

The PAICE software (Paice_v2_90.jar) http://sourceforge.net/projects/paice/ (Hosseini et al. unpublished) was developed for the pathway analyses. The PAICE software visualizes pathways according to Kyoto Encyclopedia of Genes and Genomes (KEGG) (http://www.genome.jp/kegg/catalog/org_list.html) from Affymetrix® gene expression data. There are 38,099 probe sets on The Affymetrix® soybean GeneChip®. As of June, 2011, 9,717 probe sets (29%) have reference pathway enzyme commission (E.C.) numbers. There are 23,583 probe sets with matches to *Arabidopsis thaliana* accessions (62%). The number of probe sets matching both *A. thaliana* accessions and having E.C. numbers is 4,156 (11%). The PAICE pathway analysis was performed according to Klink et al. (2011) using a modified version for data obtained through the DCM. Data supplemental to each table and figure and GO terms (Harris et al. 2004) are provided. The seven supplemental datasets (Supplemental Datasets 1–7) can be found at the website: http://dl.dropbox.com/u/428435/DCM%20PATHWAYS.zip.

Chromosomal map coordinates

The Genbank accessions of probe sets on the Affymetrix® soybean GeneChip® (Supplemental table 1) were queried against the sequences *G. max*$_{[\text{Williams 82/PI 518671}]}$ (Supplemental table 2) (Schmutz et al. 2010) genome at http://www.phytozome.org/. The queries were performed in the *Glycine max* database using the Blast option. Once the chromosomal map coordinates were obtained, the coordinates were queried into http://www.soybase.org, allowing for the identification of the microarray-identified genes and their chromosomal map coordinates to physical map positions in relation to the genetic positions of the resistance loci.

Results

Intergenotype analyses identify genes that are expressed in a genotype-dependent manner

Detection call methodology (DCM) was used to compare the *G. max*$_{[\text{Peking/PI 548402}]}$ and *G. max*$_{[\text{PI 88788}]}$ defense responses using the Affymetrix® GeneChip fabricated with 38,099 soybean probe sets. Comparisons were made at the 3 dpi time point syncytia (Fig. 3a; Supplemental table 3), 6 dpi (Fig. 3b; Supplemental table 4) and 9 dpi time points (Fig. 3c; Supplemental table 5). The analyses of the combined data from the 3, 6 and 9 dpi time points demonstrate that *G. max*$_{[\text{Peking/PI 548402}]}$ and *G. max*$_{[\text{PI 88788}]}$ are undergoing gene expression that is different from syncytia undergoing the susceptible reaction (Fig. 3d; Supplemental table 6). Expression was confirmed using Illumina® deep sequencing platform (Table 1; Supplemental table 7).

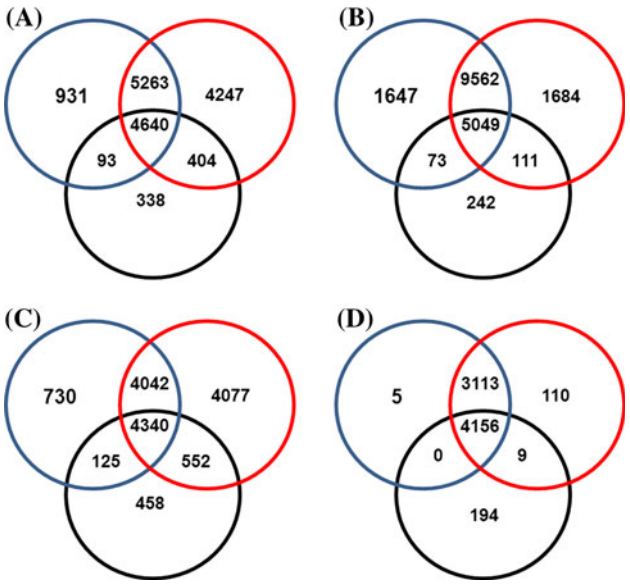

Fig. 3 Intergenotype analyses represented by Venn diagrams depicting the four comparative analyses made between the *G. max*$_{[Peking/PI\ 548402]}$ resistant syncytium (*blue circle*), *G. max*$_{[PI\ 88788]}$ resistant syncytium (*red circle*) and *G. max*$_{[Peking/PI\ 548402]}$ susceptible time course (*black circle*). The *blue ring* represents the *G. max*$_{[Peking/PI\ 548402]}$ resistant syncytium pools of genes. The *red ring* represents the *G. max*$_{[PI\ 88788]}$ resistant syncytium pool of genes. The *black ring* represents the *G. max*$_{[Peking/PI\ 548402]}$ susceptible syncytium time course pool of genes. **a** 3 dpi *G. max*$_{[Peking/PI\ 548402]}$ and *G. max*$_{[PI\ 88788]}$ resistant syncytium samples compared to *G. max*$_{[Peking/PI\ 548402]}$ susceptible syncytium time course pool of genes. **b** 6 dpi *G. max*$_{[Peking/PI\ 548402]}$ and *G. max*$_{[PI\ 88788]}$ resistant syncytium samples compared to *G. max*$_{[Peking/PI\ 548402]}$ susceptible syncytium time course pool of genes. **c** 9 dpi *G. max*$_{[Peking/PI\ 548402]}$ and *G. max*$_{[PI\ 88788]}$ resistant syncytium sample pool compared to *G. max*$_{[Peking/PI\ 548402]}$ susceptible syncytium pool of genes. **d** Combined 3, 6 and 9 dpi *G. max*$_{[Peking/PI\ 548402]}$ and *G. max*$_{[PI\ 88788]}$ resistant syncytium sample pool compared to *G. max*$_{[Peking/PI\ 548402]}$ susceptible syncytium time course pool of genes

Time point analyses identify genes that pertain to defense

Experiments were then designed to determine gene expression that is common to *G. max*$_{[Peking/PI\ 548402]}$ and *G. max*$_{[PI\ 88788]}$ syncytia as they undergo their respective defense responses. Experimental data are presented here only from genes that are present in all replicates for a particular cell type of both genotypes (*G. max*$_{[Peking/PI\ 548402+PI\ 88788]}$) undergoing their defense responses (Fig. 4). The analyses of the 3 dpi time point demonstrate that *G. max*$_{[Peking/PI\ 548402+PI\ 88788]}$ syncytia undergo gene expression that is different from both pericycle and the surrounding cells as well as syncytia undergoing the susceptible reaction (Fig. 4a; Supplemental table 8). The analyses were followed by examining expression occurring at 6 dpi (Fig. 4b; Supplemental table 9) and 9 dpi (Fig. 4c; Supplemental table 10). Combining data from the 3, 6 and 9 dpi time points

Table 1 Illumina® deep sequencing experiment for the *G. max*$_{[PI\ 88788]}$ 9 dpi resistant reaction time point

AFFYMETRIX probe set	Chromosomal location	Illumina: % of tags*
Gma.3940.1.S1_at	Glyma13g06450.1	17.3967
Gma.16471.1.S1_at	Glyma17g07250.1	11.66824
Gma.6290.1.S1_at	Glyma14g07460.1	9.966236
GmaAffx.21298.1.S1_at	Glyma13g25020.1	9.796265
GmaAffx.93619.1.S1_s_at	Glyma12g33530.1	7.118084
Gma.10919.2.S1_s_at	Glyma03g35180.2	6.697751
GmaAffx.88992.1.A1_at	Glyma20g05560.1	5.64807
GmaAffx.11803.1.A1_at	Glyma11g11240.1	3.805958
GmaAffx.87597.1.S1_at	Glyma10g07450.1	3.126077
Gma.13476.1.A1_at	Glyma08g03130.1	1.846705
GmaAffx.34450.1.S1_at	Glyma05g05290.1	1.529733
Gma.9307.1.S1_at	Glyma12g35990.1	1.442451
GmaAffx.2269.1.S1_at	Glyma02g11060.1	1.120886
Gma.10632.1.S1_a_at	Glyma04g43160.1	1.070354
GmaAffx.90320.1.S1_s_at	Glyma17g23870.1	0.856743
GmaAffx.89786.1.S1_at	Glyma13g12070.1	0.542068
GmaAffx.1332.1.S1_at	Glyma11g01070.1	0.537474
GmaAffx.65693.2.S1_s_at	Glyma09g33650.1	0.39966
Gma.12624.1.S1_at	Glyma13g39120.1	0.383582
GmaAffx.74918.1.S1_at	Glyma02g41490.1	0.298597
GmaAffx.89726.1.A1_s_at	Glyma13g42330.1	0.243471
GmaAffx.53904.1.S1_at	Glyma18g48350.1	0.218205
GmaAffx.90263.1.S1_s_at	Glyma07g00900.2	0.192939
GmaAffx.86757.1.S1_at	Glyma02g25950.1	0.179158
GmaAffx.82344.1.S1_at	Glyma12g34570.2	0.156189
Gma.11106.2.S1_at	Glyma06g02990.1	0.142408
GmaAffx.89861.1.A1_at	Glyma20g27940.1	0.126329
Gma.6533.1.S1_at	Glyma17g37400.1	0.124032
Gma.4999.1.S1_s_at	Glyma08g46240.1	0.117142
GmaAffx.60419.1.S1_x_at	Glyma17g23900.1	0.110251
GmaAffx.35639.1.A1_at	Glyma01g35480.1	0.107954
Gma.3881.1.S1_s_at	Glyma02g40290.2	0.105657
GmaAffx.89225.1.S1_s_at	Glyma17g02260.1	0.105657
Gma.2590.1.A1_s_at	Glyma10g35870.2	0.101064
Gma.443.1.S1_at	Glyma08g18130.1	0.091876
Gma.6664.2.S1_at	Glyma19g37000.1	0.091876
Gma.11247.1.S1_at	Glyma08g41060.1	0.089579
GmaAffx.89113.1.S1_x_at	Glyma03g34310.1	0.089579
Gma.5947.1.S1_s_at	Glyma09g04530.1	0.084985
GmaAffx.1301.92.S1_s_at	Glyma13g12020.1	0.080391
Gma.1034.4.S1_s_at	Glyma17g18800.1	0.073501
GmaAffx.92561.1.S1_s_at	Glyma16g07750.1	0.068907
Gma.4189.1.S1_at	Glyma17g01720.1	0.059719
GmaAffx.81963.1.S1_at	Glyma16g19560.1	0.059719
Gma.1079.1.S1_s_at	Glyma08g11480.1	0.059719
GmaAffx.89772.14.A1_s_at	Glyma17g03350.1	0.057422
GmaAffx.34785.9.S1_at	Glyma13g11930.1	0.057422

Table 1 continued

AFFYMETRIX probe set	Chromosomal location	Illumina: % of tags*
Gma.15478.2.S1_at	Glyma17g04340.1	0.057422
GmaAffx.90331.1.S1_s_at	Glyma08g24760.1	0.055126
Gma.16887.2.S1_at	Glyma04g08200.1	0.055126
GmaAffx.89703.1.A1_at	Glyma12g07780.3	0.050532
GmaAffx.92028.1.S1_at	Glyma10g01080.1	0.050532
GmaAffx.29710.1.S1_at	Glyma18g53470.1	0.048235
Gma.11179.1.S1_s_at	Glyma03g32850.1	0.048235
GmaAffx.92063.1.S1_s_at	Glyma17g01500.1	0.048235
Gma.17595.1.S1_s_at	Glyma18g44850.1	0.045938
GmaAffx.93164.1.S1_s_at	Glyma18g39690.1	0.045938
Gma.2133.1.S1_at	Glyma10g30110.1	0.045938
Gma.756.2.S1_s_at	Glyma15g08300.1	0.043641
GmaAffx.1301.58.S1_s_at	Glyma15g19580.1	0.043641
Gma.1634.1.S1_at	Glyma12g10150.2	0.043641
Gma.8449.1.S1_s_at	Glyma11g01240.1	0.043641
GmaAffx.83146.1.S1_s_at	Glyma17g35720.1	0.043641
Gma.2655.2.S1_a_at	Glyma12g16560.1	0.041344
GmaAffx.15940.1.S1_at	Glyma17g14750.1	0.041344
Gma.11179.3.S1_x_at	Glyma19g35560.1	0.039047
GmaAffx.89705.1.S1_s_at	Glyma04g01130.2	0.039047
GmaAffx.91487.1.S1_x_at	Glyma05g11630.1	0.039047
GmaAffx.89781.1.S1_s_at	Glyma12g00390.1	0.039047
GmaAffx.25068.1.A1_s_at	Glyma02g47960.1	0.039047
GmaAffx.42055.1.S1_at	Glyma17g13510.1	0.039047
Gma.10990.2.S1_x_at	Glyma11g11900.1	0.03675
Gma.5129.1.S1_at	Glyma11g18320.1	0.03675
GmaAffx.87207.1.S1_at	Glyma06g19890.1	0.03675
Gma.2892.2.S1_at	Glyma06g08380.1	0.03675
Gma.17525.1.S1_at	Glyma18g08220.1	0.034454
GmaAffx.78601.1.S1_s_at	Glyma12g08040.1	0.034454
Gma.10969.1.S1_a_at	Glyma13g42340.1	0.034454
Gma.10988.3.S1_x_at	Glyma14g09440.1	0.034454
Gma.17594.2.S1_at	Glyma10g31590.1	0.034454
Gma.11130.2.S1_at	Glyma12g29510.2	0.032157
GmaAffx.90275.1.S1_at	Glyma08g13130.1	0.032157
GmaAffx.89946.1.S1_x_at	Glyma16g28590.1	0.032157
GmaAffx.93348.1.S1_at	Glyma15g40860.1	0.032157
GmaAffx.84025.1.S1_at	Glyma01g41460.1	0.032157
Gma.8141.1.A1_at	Glyma09g33680.1	0.032157
Gma.186.1.S1_at	Glyma15g32800.1	0.02986
GmaAffx.1301.131.A1_x_at	Glyma05g25810.1	0.02986
Gma.17610.1.S1_x_at	Glyma15g03050.1	0.02986
GmaAffx.93032.1.S1_s_at	Glyma03g28410.2	0.02986
Gma.3893.1.S1_at	Glyma08g05610.2	0.02986
Gma.11037.1.S1_at	Glyma16g04940.1	0.02986
Gma.7112.1.S1_a_at	Glyma16g21590.2	0.02986
Gma.2266.1.S1_s_at	Glyma10g06600.1	0.02986
GmaAffx.90998.1.S1_s_at	Glyma05g24110.1	0.02986

Table 1 continued

AFFYMETRIX probe set	Chromosomal location	Illumina: % of tags*
GmaAffx.497.1.S1_at	Glyma13g19330.1	0.027563
GmaAffx.82418.1.S1_x_at	Glyma20g34880.1	0.027563
Gma.2313.1.S1_s_at	Glyma10g38760.1	0.027563
GmaAffx.50338.1.S1_at	Glyma10g39450.1	0.027563
Gma.5451.1.S1_at	Glyma02g15190.1	0.027563

Gene annotation	KEGG annotation
Unknown	
XYLOGLUCAN ENDOTRANSGLYCOSYLASE 6 (XTR6)	2.4.1.207
BOTRYTIS-INDUCED KINASE1 (BIK1)	–
Dentin phosphoryn protein	–
Fasciclin-like arabinogalactan protein 9.2	–
Zinc finger (AN1-like) family protein	–
Conserved hypothetical	–
Eukaryotic initiation factor 4B-like	–
Phloem protein 2-A15 (ATPP2-A15)	–
Hua enhancer 2 (HEN2) RNA helicase IN	–
Bax inhibitor-like protein	–
Bax inhibitor-like protein	–
AP2/EREBP-mediated defense pathway	K09287
Ubiquitin-fold modifier 1-like (Ufm1)	K12162
Conserved hypothetical	–
Conserved hypothetical	–
Predicted protein	–
Phosphoenolpyruvate carboxykinase	–
Predicted protein	–
APK1A (Arabidopsis protein kinase 1A)	–
LIPOXYGENASE 1 (LOX1)	1.13.11.12
Peptidyl-prolyl cis–trans isomerase	–
Seed lipoxygenase	1.13.11.12
Bet v I allergen family protein	–
Sali3-2	–
MADS-box protein	K09264
Ubiquitin C variant	–
Cysteine proteinase precursor	3.4.22.-
Wound-induced basic protein	–
No match	–
No match	–
Trans-cinnamate 4-monooxygenase	1.14.13.11
Diamine oxidase	–
Predicted protein	–

Table 1 continued

Gene annotation	KEGG annotation
Myb, DNA-binding; Glycosyl transferase, group 1	2.4.1.142
Nodulin-26	K09873
ATHVA22C	–
Nodulin-26	K09873
Pathogenesis-related class 10 protein SPE-16	–
Cytochrome P450 monooxygenase	–
Caffeoyl-CoA O-methyltransferase	–
Predicted protein	–
Cationic peroxidase 2	1.11.1.7
Phototropin	–
Adenosylhomocysteinase	–
PR10-like protein	–
Conserved hypothetical	–
S-ADENOSYLMETHIONINE SYNTHETASE 2 (SAM-2)	–
Bet v I family protein	–
Proteasome subunit beta type-6	3.4.25.1
L-ascorbate peroxidase, cytosolic	–
RAD5-DNA repair	–
RAD23-DNA repair	K10839
HEAT SHOCK COGNATE PROTEIN 70-1 (HSC70-1)	K03283
Aspartic proteinase 1	3.4.23.40
UBIQUITIN CONJUGATING ENZYME 8 (UBC8)	–
Type 2 metallothionein	–
Alcohol acyl-transferases	–
Auxin-repressed protein	–
Cysteine protease	–
DnaJ seed maturation protein PM37	–
4-coumarate:CoA ligase isoenzyme 3	6.2.1.12
Cysteine proteinase precursor	–
IAA-LEUCINE RESISTANT3 (ILR3) bHLH transcription factor	–
Beta-fructosidase (BFRUCT3)	3.2.1.26
Heat shock protein 70 (HSP70)	K03283
ERD14	–
Elongation factor 1-alpha	–
Patellin-3; SEC14 homolog	–
Chlorophyll a-b binding protein 8	–
Esterase/lipase/thioesterase	–
Fructose-bisphosphate aldolase-phosphate shunt	4.1.2.13
Pyridine nucleotide-disulphide oxidoreductase family protein	–
ENHANCED DISEASE SUSCEPTIBILITY 1 (EDS1)	–

Table 1 continued

Gene annotation	KEGG annotation
26S proteasome regulatory particle non-ATPase subunit6	K03036
HEAT SHOCK PROTEIN 81-2 (HSP81-2)	K04079
Aquaporin PIP2,2	–
LIPOXYGENASE 1 (LOX1)	1.13.11.12
Cysteine proteinase precursor	3.4.22.-
ARABIDOPSIS THALIANA METHIONINE GAMMA-LYASE (ATMGL)	4.4.1.11
PLASMA MEMBRANE INTRINSIC PROTEIN 2;4 (PIP2;4)	K09872
Conserved hypothetical	–
No match	–
Elongation factor 1	3.6.5.3
Polycomb group protein EMF2	–
Sugar transporter/spinster transmembrane protein	–
SOS3-INTERACTING PROTEIN 3 (SIP3)	–
Photosystem II light harvesting complex gene 1.4	K08912
LIPOXYGENASE 1 (LOX1)	1.13.11.12
Ferredoxin-dependent glutamate synthase	1.4.7.1
Receptor for activated protein kinase C (RACK1)	–
GLYCERALDEHYDE 3-PHOSPHATE DEHYDROGENASE A SUBUNIT (GAPA)	1.2.1.13
RNA polymerase I specific transcription initiation factor	–
Cell wall-associated hydrolase-homologous to bacterial proteins	–
Elongation factor 1A	–
Heat shock cognate 70 kDa protein 1	K03283
DAG putative plastid developmental protein	–
ATP sulfurylase 2 APS3)	2.7.7.4
Haloacid dehalogenase-like hydrolase family protein	–
RNA-binding protein 47B	–

demonstrate a core set of constitutively and perhaps uniquely active genes in *G. max*$_{[\text{Peking/PI 548402+PI 88788}]}$ syncytia undergoing their defense responses (Fig. 4d; Supplemental table 11). Analyses presented in Fig. 4d show that 1,787 probe sets, representing ~5% of the total array, measure expression specifically in *G. max*$_{[\text{Peking/PI 548402+PI 88788}]}$ syncytia throughout defense.

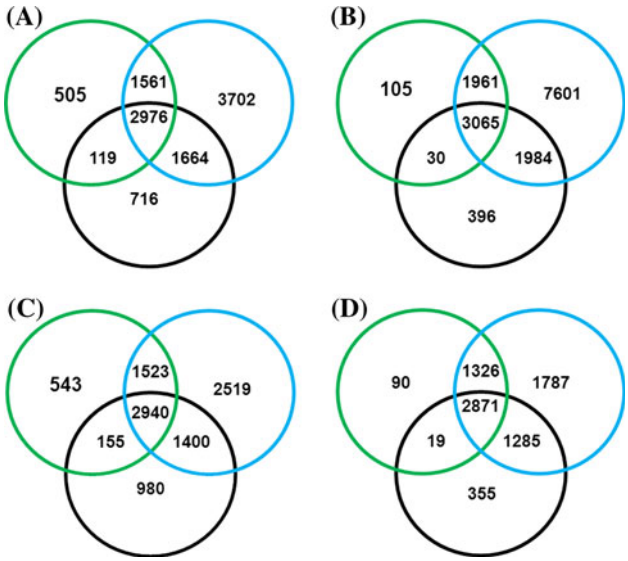

Fig. 4 Time point analyses represented by Venn diagrams depicting the four comparative analyses made between the *G. max*$_{[Peking/PI\ 548402+PI\ 88788]}$ pericycle and surrounding cells, the *G. max*$_{[Peking/PI\ 548402+PI\ 88788]}$ defense response and the *G. max*$_{[Peking/PI\ 548402]}$ susceptible reaction. The *green ring* represents the *G. max*$_{[Peking/PI\ 548402+PI\ 88788]}$ pericycle and surrounding cells pool of genes. The *light blue ring* represents the *G. max*$_{[Peking/PI\ 548402+PI\ 88788]}$ syncytium defense response pool of genes. The *black ring* represents the *G. max*$_{[Peking/PI\ 548402]}$ susceptible syncytium pool of genes during a time course of infection. **a** Comparative analysis of 3 dpi *G. max*$_{[Peking/PI\ 548402+PI\ 88788]}$ resistant reaction to *G. max*$_{[Peking/PI\ 548402+PI\ 88788]}$ pericycle and the *G. max*$_{[Peking/PI\ 548402+PI\ 88788]}$ and *G. max*$_{[Peking/PI\ 548402]}$ susceptible reaction sample pool of genes. **b** Comparative analysis of 6 dpi *G. max*$_{[Peking/PI\ 548402+PI\ 88788]}$ defense response to *G. max*$_{[Peking/PI\ 548402+PI\ 88788]}$ pericycle and the *G. max*$_{[Peking/PI\ 548402+PI\ 88788]}$ and *G. max*$_{[Peking/PI\ 548402]}$ susceptible reaction sample pool of genes. **c** Comparative analysis of 9 dpi *G. max*$_{[Peking/PI\ 548402+PI\ 88788]}$ defense response to *G. max*$_{[Peking/PI\ 548402+PI\ 88788]}$ pericycle and the *G. max*$_{[Peking/PI\ 548402+PI\ 88788]}$ and *G. max*$_{[Peking/PI\ 548402]}$ susceptible reaction sample pool. **d** Comparative analysis of 3, 6 and 9 dpi *G. max*$_{[Peking/PI\ 548402+PI\ 88788]}$ defense response to *G. max*$_{[Peking/PI\ 548402+PI\ 88788]}$ pericycle and the *G. max*$_{[Peking/PI\ 548402+PI\ 88788]}$ and *G. max*$_{[Peking/PI\ 548402]}$ susceptible reaction sample pool

Intergenotype PAICE analyses reveal genotype-specific metabolic pathway activity

PAICE (Hosseini et al. unpublished) was developed to place the expressed genes into their metabolic context (Table 2). The pathways that are identified in the resistant reactions of *G. max*$_{[Peking/PI\ 548402]}$, *G. max*$_{[PI\ 88788]}$, the susceptible reaction and those found in all three cell types for pericycle (Supplemental dataset 1), 3 dpi (Supplemental dataset 2) 6 dpi (Supplemental dataset 3) and 9 dpi comparisons (Supplemental dataset 4) are provided. The analyses reveal that while commonalities exist in gene activity for hundreds of pathways between *G. max*$_{[Peking/PI\ 548402]}$ and *G. max*$_{[PI\ 88788]}$, specific alterations in expression exist

Table 2 PAICE pathway count for the intergenotype analyses accompanying Fig. 3

Comparison	Peking	PI 88788	Susceptible	Common	Total
Pericycle	45	133	N/A	121	299
3 dpi	38	99	15	90	242
6 dpi	50	48	13	94	205
9 dpi	33	92	24	90	239
Total					985

that accompany the distinct forms of their genotype-defined defense responses (Fig. 5).

Time point PAICE pathway analyses identify syncytium-specific expression

PAICE was then used to analyze the pooled transcript data obtained from *G. max*$_{[Peking/PI\ 548402+PI\ 88788]}$ syncytia undergoing their defense responses at 3, 6 and 9 dpi to *G. max*$_{[Peking/PI\ 548402+PI\ 88788]}$ to both pericycle and their surrounding cells and syncytia undergoing the susceptible reaction. The time point analyses resulted in the generation of a total of 658 PAICE pathways (Table 3). Removing duplicate pathways occurring in the different time points and cell types resulted in the identification of 119 pathways with gene expression activity (Fig. 6).

Time point analyses identify genes found at the *rhg1* locus that are expressed in the syncytium during defense

The time point PAICE analyses are designed to visualize metabolic activity for all genes exhibiting expression. Gene activity at the *rhg1* locus can be measured by the 112 probe sets fabricated onto the array that represent the locus (Supplemental table 12). Expression studies show that 18 of the 112 probe sets spanning the *rhg1* locus are measuring expression in at least one sample at the studied time points (Fig. 7). The gene lists for the 3 dpi (Supplemental dataset 5) 6 dpi (Supplemental dataset 6) and 9 dpi time points (Supplemental dataset 7) are provided. In sum, two adjacent genes within the 67 kb *rhg1* region had expression only in syncytia undergoing defense and at all time points as revealed by the experimental conditions (Fig. 7).

Discussion

An analysis of gene expression of soybean germplasm obtained originally from ecological collections was used to show how natural genetic variation is a useful tool in understanding defense at cellular resolution. The study

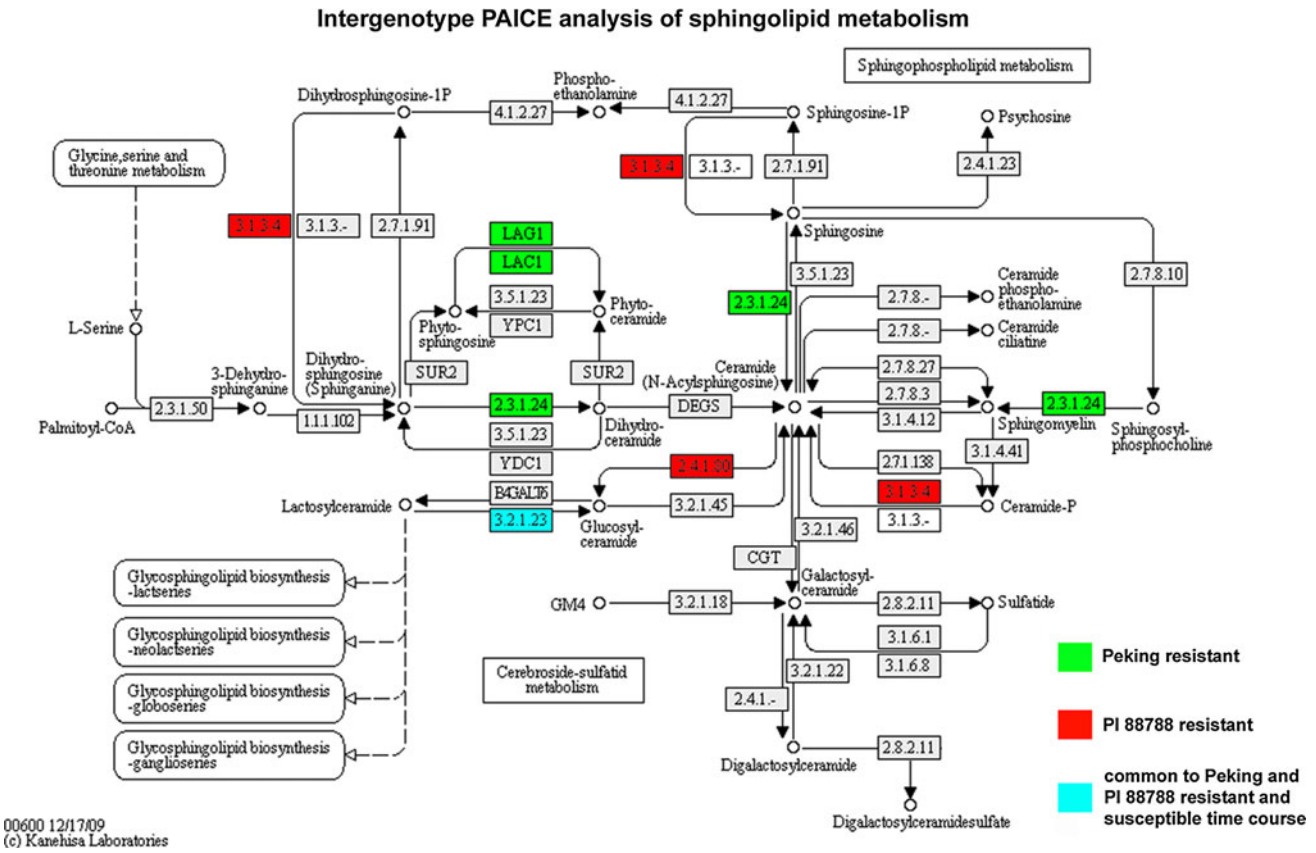

Fig. 5 Intergenotype PAICE analysis of sphingolipid metabolism, map 00600. Probe sets detecting expression for Peking resistant reaction at 9 dpi (*green*); PI 88788 resistant reaction at 9 dpi (*red*); Peking resistant reaction at 9 dpi, PI 88788 resistant reaction at 9 dpi and the susceptible time course (*blue*). *Note* No expression was found for sphingolipid metabolism that was limited only to the susceptible time course

Table 3 PAICE pathway count for the time point analyses accompanying Fig. 4

Comparison	Susceptible syncytia	Resistant syncytia	Pericycle	Common	Total
3 dpi	41	86	29	69	225
6 dpi	22	108	6	71	207
9 dpi	49	78	28	71	226
Total					658

generated a map of cell fate decisions as soybean was undergoing infection leading to either a susceptible reaction or a successful defense response to SCN infection. The analysis presented here was accomplished by examining gene expression occurring at the site of infection, the syncytium. Notably, the genes focused in on here do not meet the statistical cut-off parameters in differential expression studies and are therefore discarded from further analysis (Klink et al. 2007, 2009). This outcome occurred because the probe sets measured expression in samples isolated from one cell type but lacked the measurement of expression in other cell types, making statistical comparisons impossible for differential expression studies. The work presented here was built off the premise that cell-type specific expression is a hallmark of cellular identity, especially during specialized processes such as defense to pathogens. The analysis presented here demonstrates that there is a basic conserved expression program in place that would likely be common to all soybean genotypes undergoing defense to SCN (Klink et al. 2011). It is on this conserved gene expression platform that genotype-specific expression is organized and orchestrated during defense to SCN (Klink et al. 2011). This expression is what governs the different cellular features that are present during the *G. max*$_{[\text{Peking/PI 548402}]}$ and *G. max*$_{[\text{PI 88788}]}$ forms of the resistant reaction. Identifying differences in gene expression at the cellular level is not unexpected and is consistent with single cell type gene expression studies done in other experimental systems undergoing a developmental process (Benfey and Mitchell-Olds 2008; Chiang and Melton 2003; Guo et al. 2011; Tang et al. 2011).

Detection calls confirmed by Illumina® deep sequencing

While the DCM provides a statistical output, it is difficult to determine what the relative quantities of a transcript are.

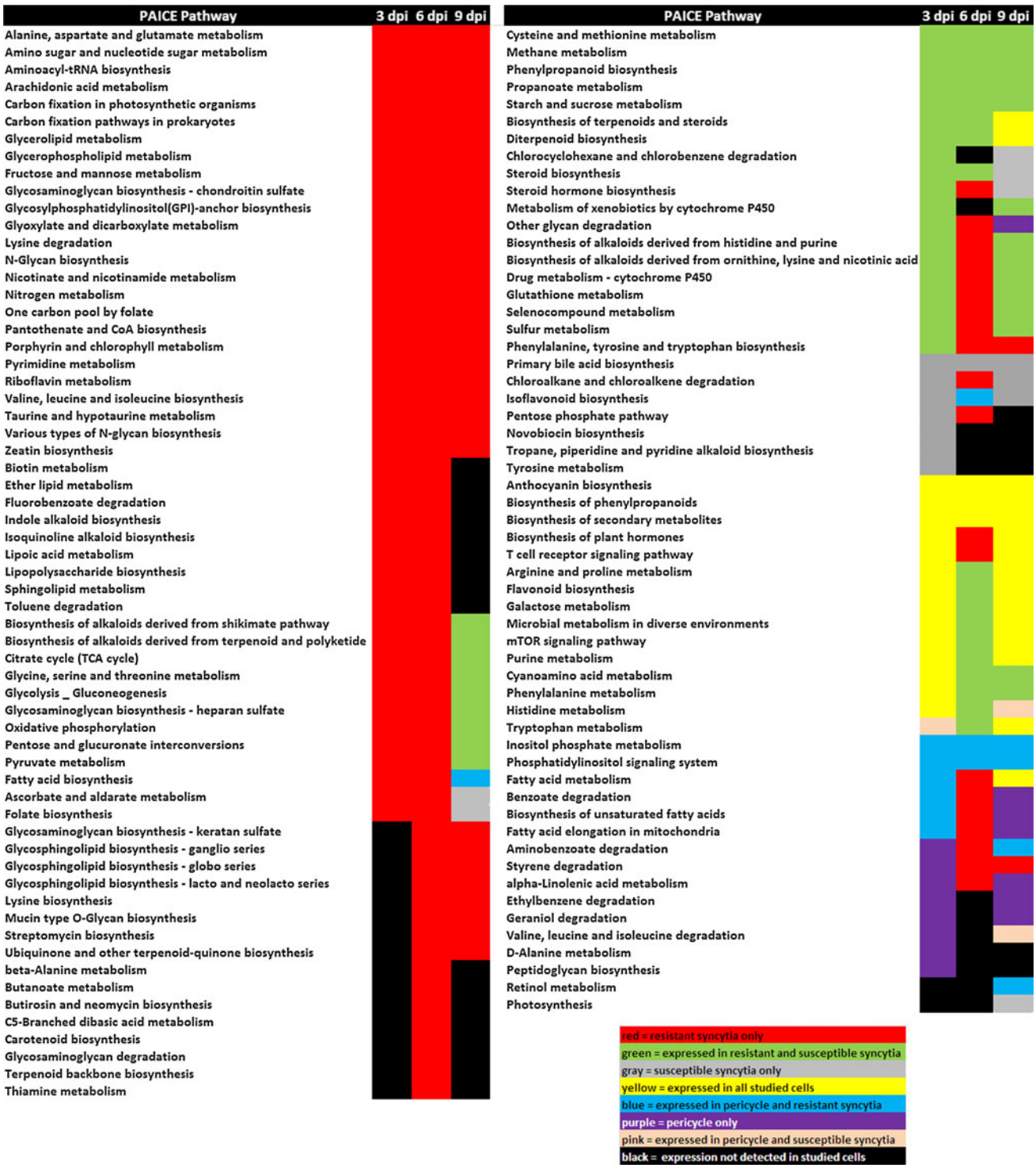

Fig. 6 PAICE pathway analyses. Pathway activity is shown for 3, 6 and 9 dpi time points. *Red* Resistant syncytia only, *green* expressed in resistant and susceptible syncytia, *gray* susceptible syncytia only, *yellow* expressed in all cell types, *blue* expressed in pericycle and resistant syncytia, *purple* pericycle only, *pink* expressed in pericycle and susceptible syncytia, *black* expression not detected in sample

It was revealed through Illumina® deep sequencing that some of these genes can be represented by a fairly large percentage of the transcripts in a sample type. For example, the Affymetrix probe set Gma.3940.1.S1_at, whose sequence is Glyma13g06450.1, is an unknown gene that does not appear to be conserved with other organisms. However, it represented over 17% of the transcripts in the 9 dpi *G. max*$_{[PI\ 88788]}$ sample isolated from cells undergoing

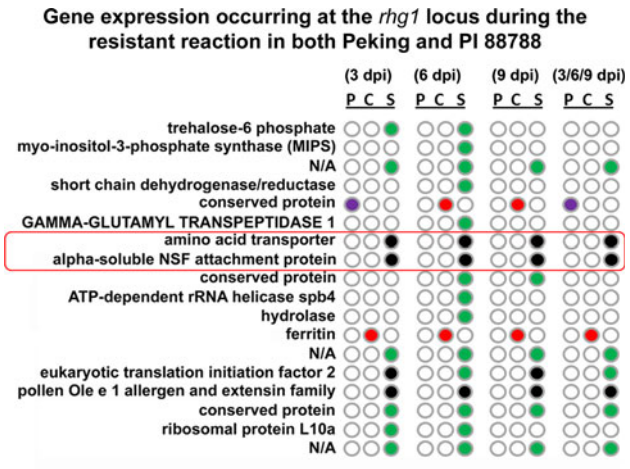

Fig. 7 Time point analyses of the *rhg1* locus. Expression is presented in relation to map positions of Affymetrix® probe sets and genes at the locus with gene activity as demonstrated. The list represents probe sets that have chromosomal coordinates on chromosome 18 in the region of *rhg1* and also have expression data. P, pericycle and surrounding cells; C, common; S, syncytium. *Purple* Pericycle; *red* expressed in pericycle and syncytium; green syncytium; *black* uniquely expressed in syncytia undergoing a defense response as compared to pericycle and syncytia undergoing a susceptible reaction. Duplicate probe sets having identical gene expression were consolidated. The *red box* represents the only genes within the 67 kb region (Kim et al. 2010) between the markers BARCSOYSSR_18_0090 and BARCSOYSSR_18_0094 that had any expression

resistance. The XYLOGLUCAN ENDOTRANSGLYCOSYLASE 6 (XTR6) gene was represented by over 11% of the transcripts. The XTRs modify the plant cell wall xyloglucan-cellulose framework and by doing so, modulate strength and expansion. This activity appears to occur at the point of formation of secondary cell walls through restructuring of the primary cell walls (Bourquin et al. 2002). Very little is understood about XTRs and defense. However, the reinforcement of cell walls is a component of defense of soybean to SCN (Mahalingham and Skorupska 1996). Another gene, BOTRYTIS-INDUCED KINASE1 (BIK1) that constituted almost 10% of the Illumina® -identified transcripts was originally identified as a defense gene (Veronese et al. 2006). BIK1 is activated within minutes after infection of *Arabidopsis thaliana* by *Botrytis cinerea* (Veronese et al. 2006; Laluk et al. in press). BIK1 has been shown to play essential roles in plant growth, ethylene signaling and pathogen activated molecular patterning (PAMP) during defense. The BIK1 protein localizes to cell membranes and it was suggested that it may act early during the interaction between the plant and pathogen (Veronese et al. 2006). Of note, the defense requirement of BIK1 functions in relation to salicylic acid levels. The addition of the Illumina® sequencing thus places the Affymetrix® detection data into an expression context since relative amounts of transcripts that are present within a sample are obtained. What is clear from the Illumina® experiments is the accuracy of the Affymetrix® detection calls.

Time point PAICE analyses

The time point PAICE analyses revealed gene activity occurring specifically during the resistant reaction. These experiments demonstrated the activity of many pathways at 3 dpi, a period when the soybean is altering its gene expression that leads to visible signs of the defense response (Ross 1958; Endo 1964, 1965; Endo and Veech 1970; Gipson et al. 1971; Jones and Northcote 1972; Riggs et al. 1973; Kim et al. 1987; Kim and Riggs 1992; Mahalingham and Skorupska 1996; Klink et al. 2007, 2009, 2010a, b). However, the expression of a pathway in cells that will undergo defense was never limited only to the 3 dpi syncytium samples. In some cases gene expression was measured in syncytia undergoing defense for the earlier 3 and 6 dpi time points while lacking any expression at the 9 dpi time point. In these cases, the analyses revealed the expression of lipoic acid metabolism that is part of a nonenzymatic antioxidant system in plant cells (Pérez-López et al. 2010) and processes leading to lipid production (Baud et al. 2007). The pathways for indole alkaloid biosynthesis (Onkokesung et al. 2010; Hanssen et al. 2011) and isoquinoline alkaloid biosynthesis (Facchini et al. 1996; Holková et al. 2010), having roles in defense, were also observed to be active. The pathway involved in the biosynthesis of glycosphingolipids was observed to be active. Glycosphingolipids are a class of sphingolipids of which there are greater than 168 in *A. thaliana* (Markham and Jaworski 2007) and perform roles in cell death. Other active pathways include the biosynthesis of alkaloids from the shikimate pathway (Zulak et al. 2008). The shikimate pathway provides metabolites for the production of phenylpropanoids that are metabolized into substances that perform defense roles. The pathway involved in the biosynthesis of alkaloids from terpenoid and polykeytides that are jasmonate regulated (Menke et al. 1999; Montiel et al. 2011) and fatty acid biosynthesis (Savchenko et al. 2010; Gao et al. 2011; Meldau et al. 2011) are also active.

Some pathways appeared to be active at all points during the defense response, including increased activity of components of the arachidonic acid pathway (Klink et al. 2011). The direct link of arachidonic acid metabolism to α-linoleic acid metabolism, shown to be differentially expressed during defense to SCN (Klink et al. 2011) provides additional support to the metabolic pathway leading to the synthesis of methyl jasmonate possibly being involved in *G. max* defense to *H. glycines* (Klink et al. 2007, 2009, 2010a). Notably, genetic data in *Zea mays* has already linked the involvement of JA signaling during its

defense of the plant parasitic nematode *Meloidogyne incognita* (Gao et al. 2008). Arachidonic acid functions in defense by triggering programmed cell death (Bostock et al. 1981, 1986). Arachdonic acid metabolism is active through genes leading to the synthesis of hydroxyepoxyeicosadienoic acid and tetrahydrofuran diols. This observation is important because experiments in other plant-pathogen systems demonstrate that furans are an important component of plant defense responses, working efficiently on inhibiting larva development of insects (Rodriguez-Saona et al. 2000). Other gene pathways that are active at the 3, 6 and 9 dpi time points include N-glycan biosynthesis (reviewed in Pattison and Amtmann, 2009) and nicotinate and nicotinamide metabolism (Steppuhn et al. 2004) perform roles in defense. The analyses also identified glycerolipid metabolism (Kachroo et al. 2004; Chaturvedi et al. 2008; Xia et al. 2010), glyoxylate and dicarboxylate metabolism (Emmerlich et al. 2003) and zeatin biosynthesis (Smigocki et al. 1993; Gális et al. 2004), pathways known to perform roles in defense.

Gene activity at the *rhg1* locus

An expression mapping analysis focused in on *rhg1*. In the time point analyses, 18 probe sets representing 18 different genes, detected expression in one or more cell types. Of those 18 probe sets, only two map within the 67 kb *rhg1* region between the markers BARCSOYSSR_18_0090 and BARCSOYSSR_18_0094 (Kim et al. 2010). The identified amino acid transporter and the α-SNAP probe sets measured expression at all of the time points (3, 6 and 9 dpi) throughout the defense response. α-SNAP, through vacuolar sorting would be considered to play a role in defense involving autophagy (Liu et al. 2005; Hofius et al. 2009). In contrast, no clear role has been determined for the amino acid transporter and defense. The lack of detection for CBL-interacting protein kinase, a conserved unknown gene, a speckle-type POZ protein-related gene, a conserved unknown gene, a cys-rich domain protein gene, an elicitor inducible protein gene and an unknown gene in pericycle and their surrounding cell samples and samples isolated from syncytia undergoing defense or the susceptible reactions are noted. However, the expression presented here only reflects what was observed under our experimental conditions.

PAICE analyses link the cytological events pertaining to resistance to genes present at the *rhg1* locus

From the studies that combined the expression data from the two genotypes, it appears that methyl jasmonate activity may be a part of a pathway that leads to transcriptional activation of genes involved in defense of soybean to the SCN. Previous reports have shown JA activity to be important in the resistance of plants to parasitic nematodes (Gao et al. 2008), supporting the transcriptomic work in *G. max* (Klink et al. 2007, 2009, 2010a). While JA activates defense pathways to many pathogens, upstream events including arachidonic acid metabolism supply metabolic products through the α-linoleic acid metabolic pathway that leads to the synthesis of 12-oxo-phytodienoic acid (OPDA) and methyl jasmonate. As already discussed, many pathways involved in lipid metabolism are observed to be expressed only in samples isolated from syncytia undergoing defense. Some of the downstream events, obvious through cytological examination of roots undergoing the defense response, include lignification and suberinization that stain readily with safranin as demonstrated by the original studies of Ross (1958) and re-examined later (Klink et al. 2009, 2010a, 2011). The synthesis of lignin and suberin is mediated through the activity of the phenylpropanoid pathway and shown to be induced in syncytia undergoing defense (Klink et al. 2007, 2009). Phenylpropanoid metabolites are involved in defense, providing a physical barrier to infection. One of the earliest structural features identified as providing a barrier against infection by some pathogens are CWAs. CWAs are present during the defense of plants to fungi (Aist 1976) and the plant parasitic nematode *H. glycines* in *G. max*$_{[Peking]}$ and *G. max*$_{[PI\ 437654]}$, but not *G. max*$_{[PI\ 88788]}$ (Kim et al. 1987; Mahalingham and Skorupska 1996). The formation of CWAs is linked to the aggregation of subcellular components at the infection site, a process that is dependent on the polarization of actin at the site of infection. The induced transcriptional activity of actin is observed in syncytia undergoing defense in *G. max*$_{[Peking/PI\ 548402]}$ (Klink et al. 2007, 2009), a soybean genotype known to have CWAs. The work of Böhlenius et al. (2010) implicates vesicular transport in CWA formation during infection of barley by *Blumeria graminis*. The experiments Böhlenius et al. (2010) relate increased production of phenylpropanoids to their delivery at localized sites in the cell at the cell wall. In related experiments, RNAi of the phenylpropanoid pathway components for monolignol biosynthesis that includes phenylalanine ammonia lyase (PAL), caffeic acid O-methyltransferase (CAOMT), caffeoyl-CoA methyltransferase (CCoAMT), and cinnamyl alcohol dehydrogenase (CAD), key components of lignin synthesis, results in super-susceptibility of wheat leaf tissues to an appropriate pathogen, *B. graminis* f. sp. tritici (Bgt) (Bhuiyan et al. 2009). All of these components have been shown induced during the defense response (Klink et al. 2007, 2009). The RNAi treatment also resulted in compromised penetration defense to a non-appropriate pathogen, *B. graminis* f. sp. Hordei (Bhuiyan et al. 2009). These observations are not surprising since CWAs are composed of materials such as lignin, pectin, suberin and chitin that are synthesized

through the phenylpropanoid pathway. It is suggested that the methyl units synthesized through S-adenosylmethionine synthetase activity in the epidermal cells at the site of infection are metabolized into CWAs (Bhuiyan et al. 2007). A link between the synthesis of the CWA component lignin and methyl units has been made. *Arabidopsis thaliana* S-methionine synthetase mutants, although appearing identical to wild type, have a 22% decrease in lignin (Shen et al. 2002). The enzyme S-methionine synthetase is found to be highly induced in syncytia undergoing a defense response in *G. max*$_{[Peking/PI\ 548402]}$ (Klink et al. 2009). Other proteins known to compose CWAs include hydroxyproline-rich glycoproteins (HRGPs) and peroxidases. The analysis of the *rhg1* region identified an extensin protein that is expressed specifically at all stages of the defense response. However, the extensin lies outside of the 67 kb *rhg1* region as defined by Kim et al. (2010). The synthesis, deposition and assembly of extensin appear to be accompanied by localized release of reactive oxygen species (ROS) including H_2O_2. The release of H_2O_2 can drive the cross-linking of proteins like extensin, directly intoxicate the pathogen and/or drive the defense response in neighboring cells (Aist 1976; Bradley et al. 1992; Levine et al. 1994; McLusky et al. 1999; Hueckelhoven et al. 1999; Mellersh et al. 2002). The activity of genes involved in H_2O_2 production is observed in syncytia undergoing a defense response (Klink et al. 2007). Many of these observations suggest altered cell wall composition being important in defense.

Conclusion

The experiments show that a vast amount of relevant gene expression data, typically representing between 5 and 20% of the genes in the soybean genome, is discarded from cell-type specific differential expression studies. Analyzing biological processes occurring in homogeneous cell types will require a modified approach that can examine the unique gene expression profiles of the different cell types and different genotypes. As shown by the Illumina® deep sequencing data, the Affymetrix® DCM profiling is accurate and should be used as an additional complimentary measure of gene activity during any biological process under study. The advantage of the quantitative Illumina® methodology, in the absence of differential expression knowledge, is that relative expression of these genes can be obtained, providing a measure of the activity of the gene in a specific cell type. The ability to map the expression to resistance loci in a genotype-dependent manner should allow for a better understanding of expression nuances that define the cellular strategies employed by the different genotypes as well as generalized expression features as they combat SCN.

Acknowledgments VPK thankfully acknowledges support provided by the Mississippi Soybean Promotion Board. Dr. Gary Lawrence, Department of Biochemistry, Molecular Biology, Entomology and Plant Pathology, Mississippi State University provided helpful insight into the developmental biology of *H. glycines* as they infect soybean and the defense responses of *G. max*$_{[Peking/PI\ 548402]}$ and *G. max*$_{[PI\ 88788]}$. VPK thanks Dr. Halina Knap, Department of Agronomy, Plant Molecular Cytogenetics and Genetics, Clemson University for crucial insights during the analyses and writing of the manuscript.

References

Acido JR, Dropkin VH, Luedders VD (1984) Nematode population attrition and histopathology of *Heterodera glycines-Soybean* associations. J Nematol 16:48–57

Aist JR (1976) Papillae and related wound plugs of plant cells. Annu Rev Phytopathol 14:145–163

Alkharouf N, Matthews BF (2004) SGMD: the soybean genomics and microarray database. Nucleic Acids Res 32:D398–D400

Alkharouf NW, Klink VP, Chouikha IB, Beard HS, MacDonald MH, Meyer S, Knap HT, Khan R, Matthews BF (2006) Timecourse microarray analyses reveals global changes in gene expression of susceptible *Glycine max* (soybean) roots during infection by *Heterodera glycines* (soybean cyst nematode). Planta 224:838–852

Bancroft I, Morgan C, Fraser F, Higgins J, Wells R, Clissold L, Baker D, Long Y, Meng J, Wang X, Liu S, Trick M (2011) Dissecting the genome of the polyploid crop oilseed rape by transcriptome sequencing. Nat Biotechnol 29:762–766

Baud S, Mendoza MS, To A, Harscoët E, Lepiniec L, Dubreucq B (2007) WRINKLED1 specifies the regulatory action of LEAFY COTYLEDON2 towards fatty acid metabolism during seed maturation in Arabidopsis. Plant J 50:825–838

Benfey PN, Mitchell-Olds T (2008) From genotype to phenotype: systems biology meets natural variation. Science 320:495–497

Bhuiyan NH, Liu W, Liu G, Selvaraj G, Wei Y, King J (2007) Transcriptional regulation of genes involved in the pathways of biosynthesis and supply of methyl units in response to powdery mildew attack and abiotic stresses in wheat. Plant Mol Biol 64:305–318

Bhuiyan NH, Selvaraj G, Wei Y, King J (2009) Gene expression profiling and silencing reveal that monolignol biosynthesis plays a critical role in penetration defence in wheat against powdery mildew invasion. J Exp Bot 60:509–521

Birnbaum K, Shasha DE, Wang JY, Jung JW, Lambert GM, Galbraith DW, Benfey PN (2003) A gene expression map of the *Arabidopsis* root. Science 302:1956–1960

Böhlenius H, Mørch SM, Godfrey D, Nielsen ME, Thordal-Christensen H (2010) The multivesicular body-localized GTPase ARFA1b/1c is important for callose deposition and ROR2 syntaxin-dependent preinvasive basal defense in barley. Plant Cell 22:3831–3844

Bostock RM, Kuc J, Laine RA (1981) Eicosapentaenoic and arachidonic acids from Phytophthora infestans elicit fungitoxic sesquiterpenes in the potato. Science 212:67–69

Bostock RM, Schaeffer DA, Hammerschmidt R (1986) Comparison of elicitor activities of arachidonic acid, fatty acids and glucans from Phytopthora infestans in hypersensitivity expression in potato tuber. Physiol Mol Plant Pathology 29:349–360

Bourquin V, Nishikubo N, Abe H, Brumer H, Denman S, Eklund M, Christiernin M, Teeri TT, Sundberg B, Mellerowicz EJ (2002) Xyloglucan endotransglycosylases have a function during the formation of secondary cell walls of vascular tissues. Plant Cell 14:3073–3088

Bradley DJ, Kjellbom P, Lamb CJ (1992) Elicitor- and wound-induced oxidative cross-linking of a proline-rich plant cell wall protein: a novel, rapid defense response. Cell 70:21–33

Brucker E, Carlson S, Wright E, Niblack T, Diers B (2005) Rhg1 alleles from soybean PI 437654 and PI 88788 respond differently to isolates of *Heterodera glycines* in the greenhouse. Theor Appl Genet 111:44–49

Caldwell BE, Brim CA, Ross JP (1960) Inheritance of resistane of soybeans to the soybean cyst nematode, *Heterodera glycines*. Agron J 52:635–636

Chaturvedi R, Krothapalli K, Makandar R, Nandi A, Sparks AA, Roth MR, Welti R, Shah J (2008) Plastid omega3-fatty acid desaturase-dependent accumulation of a systemic acquired resistance inducing activity in petiole exudates of *Arabidopsis thaliana* is independent of jasmonic acid. Plant J 54:106–117

Chiang MK, Melton DA (2003) Single-cell transcript analysis of pancreas development. Dev Cell 4:383–393

Colgrove AL, Niblack TL (2008) Correlation of female indices from virulence assays on inbred lines and field populations of *Heterodera glycines*. J Nematol 40:39–45

Concibido VC, Denny RL, Boutin SR, Hautea R, Orf JH, Young ND (1994) DNA marker analysis of loci underlying resistance to soybean cyst nematode (*Heterodera glycines* Ichinohe). Crop Sci 34:240–246

Concibido VC, Diers BW, Arelli PR (2004) A decade of QTL mapping for cyst nematode resistance in soybean. Crop Sci 44:1121–1131

Creech JE, Johnson WG (2006) Survey of broadleaf winter weeds in Indiana production fields infested with soybean cyst nematode (*Heterodera glycines*). Weed Technol 20:1066–1075

Cregan PB, Mudge J, Fickus EW, Danesh D, Denny R, Young ND (1999) Two simple sequence repeat markers to select for soybean cyst nematode resistance conditioned by the rhg1 locus. Theor Appl Genet 99:811–818

Emmerlich V, Linka N, Reinhold T, Hurth MA, Traub M, Martinoia E, Neuhaus HE (2003) Proc Natl Acad Sci USA 100:11122–11126

Endo BY (1964) Penetration and development of *Heterodera glycines* in soybean roots and related and related anatomical changes. Phytopathology 54:79–88

Endo BY (1965) Histological responses of resistant and susceptible soybean varieties, and backcross progeny to entry development of *Heterodera glycines*. Phytopathology 55:375–381

Endo BY, Veech JA (1970) Morphology and histochemistry of soybean roots infected with *Heterodera glycines*. Phytopathology 60:1493–1498

Epps JM, Chambers AY (1958) New host records for *Heterodera glycines* including one in the Labiate. Plant Dis Rep 42:194

Epps JM, Hartwig EE (1972) Reaction of soybean varieties and strains to soybean cyst nematode. J Nematol 4:222

Facchini PJ, Johnson AG, Poupart J, de Luca V (1996) Uncoupled defense gene expression and antimicrobial alkaloid accumulation in elicited opium poppy cell cultures. Plant Physiol 111:687–697

Gális I, Smith JL, Jameson PE (2004) Salicylic acid-, but not cytokinin-induced, resistance to WClMV is associated with increased expression of SA-dependent resistance genes in Phaseolus vulgaris. J Plant Physiol 161:459–466

Gao X, Starr J, Göbel C, Engelberth J, Feussner I, Tumlinson J, Kolomiets M (2008) Maize 9-Lipoxygenase ZmLOX3 controls development, root-specific expression of defense genes, and resistance to root-knot nematodes. MPMI 21:98–109

Gao QM, Venugopal S, Navarre D, Kachroo A (2011) Low oleic acid-derived repression of jasmonic acid-inducible defense responses requires the WRKY50 and WRKY51 proteins. Plant Physiol 155:464–476

Gipson I, Kim KS, Riggs RD (1971) An ultrastructural study of syncytium development in soybean roots infected with *Heterodera glycines*. Phytopathology 61:347–353

Guo G, Huss M, Tong GQ, Wang C, Sun LL, Clarke ND, Paul Robson P (2011) Resolution of cell fate decisions revealed by single-cell gene expression analysis from zygote to blastocyst. Dev Cell 18:675–685

Hanssen IM, Peter van Esse H, Ballester AR, Hogewoning SW, Parra NO, Paeleman A, Lievens B, Bovy AG, Thomma BP (2011) Differential tomato transcriptomic responses induced by pepino mosaic virus isolates with differential aggressiveness. Plant Physiol 156:301–318

Hardham AR, Takemoto D, White RG (2008) Rapid and dynamic subcellular reorganization following mechanical stimulation of Arabidopsis epidermal cells mimics responses to fungal and oomycete attack. BMC Plant Biol 8:63

Harris MA, Clark J, Ireland A, Lomax J, Ashburner M, Foulger R, Eilbeck K, Lewis S, Marshall B, Mungall C, Richter J, Rubin GM, Blake JA, Bult C, Dolan M, Drabkin H, Eppig JT, Hill DP, Ni L, Ringwald M, Balakrishnan R, Cherry JM, Christie KR, Costanzo MC, Dwight SS, Engel S, Fisk DG, Hirschman JE, Hong EL, Nash RS, Sethuraman A, Theesfeld CL, Botstein D, Dolinski K, Feierbach B, Berardini T, Mundodi S, Rhee SY, Apweiler R, Barrell D, Camon E, Dimmer E, Lee V, Chisholm R, Gaudet P, Kibbe W, Kishore R, Schwarz EM, Sternberg P, Gwinn M, Hannick L, Wortman J, Berriman M, Wood V, de la Cruz N, Tonellato P, Jaiswal P, Seigfried T, White R; Gene Ontology Consortium (2004) The gene ontology (GO) database and informatics resource. Nucleic Acids Res 32:D 258–261

Hofius D, Schultz-Larsen T, Joensen J, Tsitsigiannis DI, Petersen NH, Mattsson O, Jørgensen LB, Jones JD, Mundy J, Petersen M (2009) Autophagic components contribute to hypersensitive cell death in Arabidopsis. Cell 137:773–783

Holková I, Bezáková L, Bilka F, Balažová A, Vanko M, Blanáriková V (2010) Involvement of lipoxygenase in elicitor-stimulated sanguinarine accumulation in Papaver somniferum suspension cultures. Plant Physiol Biochem 48:887–892

Hueckelhoven R, Fodor J, Preis C, Kogel K-H (1999) Hypersensitive cell death and papilla formation in barley attacked by the powdery mildew fungus are associated with hydrogen peroxide but not with salicylic acid accumulation. Plant Physiol 119:1251–1260

Hyten DL, Choi IY, Song Q, Shoemaker RC, Nelson RI, Costa JM, Specht JE, Cregan PB (2010) Highly variable patterns of linkage disequilibrium in multiple soybean populations. Genetics 175:1937–1944

Jones MGK, Northcote DH (1972) Nematode-induced syncytium-a multinucleate transfer cell. J Cell Sci 10:789–809

Kachroo A, Venugopal SC, Lapchyk L, Falcone D, Hildebrand D, Kachroo P (2004) Oleic acid levels regulated by glycerolipid metabolism modulate defense gene expression in Arabidopsis. Proc Natl Acad Sci USA 101:5152–5157

Kim KS, Riggs RD (1992) Cytopathological reactions of resistant soybean plants to nematode invasion. In: Wrather JA, Riggs RD (eds) Biology and management of the soybean cyst nematode. APS Press, St. Paul, pp 157–168

Kim YH, Riggs RD, Kim KS (1987) Structural changes associated with resistance of soybean to *Heterodera glycines*. J Nematol 19:177–187

Kim M, Hyten DL, Bent AF, Diers BW (2010) Fine mapping of the SCN resistance locus *rhg1-b* from PI 88788. Plant Genome 3:81–89

Klink VP, MacDonald M, Alkharouf N, Matthews BF (2005) Laser capture microdissection (LCM) and expression analyses of *Glycine max* (soybean) syncytium containing root regions

formed by the plant pathogen *Heterodera glycines* (soybean cyst nematode). Plant Mol Biol 59:969–983

Klink VP, Overall CC, Alkharouf N, MacDonald MH, Matthews BF (2007) Laser capture microdissection (LCM) and comparative microarray expression analysis of syncytial cells isolated from incompatible and compatible soybean roots infected by soybean cyst nematode (*Heterodera glycines*). Planta 226:1389–1409

Klink VP, Hosseini P, Matsye P, Alkharouf N, Matthews BF (2009) A gene expression analysis of syncytia laser microdissected from the roots of the *Glycine max* (soybean) genotype PI 548402 (Peking) undergoing a resistant reaction after infection by *Heterodera glycines* (soybean cyst nematode). Plant Mol Biol 71:525–567

Klink VP, Hosseini P, Matsye P, Alkharouf N, Matthews BF (2010a) Syncytium gene expression in *Glycine max*$_{[PI\ 88788]}$ roots undergoing a resistant reaction to the parasitic nematode *Heterodera glycines*. Plant Physiol Biochem 48:176–193

Klink VP, Overall CC, Alkharouf N, MacDonald MH, Matthews BF (2010b) Microarray detection calls as a means to compare transcripts expressed within syncytial cells isolated from incompatible and compatible soybean (*Glycine max*) roots infected by the soybean cyst nematode (*Heterodera glycines*). J Biomed Biotechnol 1–30

Klink VP, Hosseini P, Matsye PD, Alkharouf N, Matthews BF (2011) Differences in gene expression amplitude overlie a conserved transcriptomic program occurring between the rapid and potent localized resistant reaction at the syncytium of the *Glycine max* genotype Peking (PI 548402) as compared to the prolonged and potent resistant reaction of PI 88788. Plant Mol Biol 75:141–165

Laluk K, Luo H, Chai M, Dhawan R, Lai Z, Mengiste T (2011) Biochemical and genetic requirements for function of the immune response regulator BOTRYTIS-INDUCED KINASE1 in plant growth, ethylene signaling, and PAMP-triggered immunity in Arabidopsis. Plant Cell [Epub ahead of print]

Lauritis JA, Rebois R, Graney LS (1983) Development of *Heterodera glycines* Ichinohe on soybean. *Glycine max* (L.) Merr., under gnotobiotic conditions. J Nematol 15:272–280

Levine A, Tenhaken R, Dixon R, Lamb C (1994) H2O2 from the oxidative burst orchestrates the plant hypersensitive disease resistance response. Cell 79:583–593

Liu Y, Schiff M, Czymmek K, Tallóczy Z, Levine B, Dinesh-Kumar SP (2005) Autophagy regulates programmed cell death during the plant innate immune response. Cell 121:567–577

Mahalingham R, Skorupska HT (1996) Cytological expression of early response to infection by *Heterodera glycines* Ichinohe in resistant PI 437654 soybean. Genome 39:986–998

Markham JE, Jaworski JG (2007) Rapid measurement of sphingolipids from *Arabidopsis thaliana* by reversed-phase high-performance liquid chromatography coupled to electrospray ionization tandem mass spectrometry. Rapid Commun Mass Spectrom 21:1304–1314

Matson AL, Williams LF (1965) Evidence of a fourth gene for resistance to the soybean cyst nematode. Crop Sci 5:477

McLusky SR, Bennett MH, Beale MH, Lewis MJ, Gaskin P, Mansfield JW (1999) Cell wall alterations and localized accumulation of feruloyl-3'- methoxytyramine in onion epidermis at sites of attempted penetration by Botrytis allii are associated with actin polarization, peroxidase activity and suppression of flavonoid biosynthesis. Plant J 17:523–534

Meldau S, Baldwin IT, Wu J (2011) SGT1 regulates wounding- and herbivory-induced jasmonic acid accumulation and Nicotiana attenuata's resistance to the specialist lepidopteran herbivore Manduca sexta. New Phytol 189:1143–1156

Mellersh DG, Foulds IV, Higgins VJ, Heath MC (2002) H2O2 plays different roles in determining penetration failure in three diverse plant–fungal interactions. Plant J 29:257–268

Menke FL, Champion A, Kijne JW, Memelink J (1999) A novel jasmonate- and elicitor-responsive element in the periwinkle secondary metabolite biosynthetic gene Str interacts with a jasmonate- and elicitor-inducible AP2-domain transcription factor, ORCA2. EMBO J 18:4455–4463

Montiel G, Zarei A, Körbes AP, Memelink J (2011) The jasmonate-responsive element from the ORCA3 promoter from Catharanthus roseus is active in Arabidopsis and is controlled by the transcription factor AtMYC2. Plant Cell Physiol 52:578–587

Mudge J, Cregan PB, Kenworthy JP, Kenworthy WJ, Orf JH, Young ND (1997) Two microsatellite markers that flank the major soybean cyst nematode resistance locus. Crop Sci 37:1611–1615

Onkokesung N, Baldwin IT, Gális I (2010) The role of jasmonic acid and ethylene crosstalk in direct defense of Nicotiana attenuata plants against chewing herbivores. Plant Signal Behav 5:1305–1307

Pattison RJ, Amtmann A (2009) N-glycan production in the endoplasmic reticulum of plants. Trends Plant Sci 14:92–99

Pérez-López U, Robredo A, Lacuesta M, Sgherri C, Mena-Petite A, Navari-Izzo F, Muñoz-Rueda A (2010) Lipoic acid and redox status in barley plants subjected to salinity and elevated CO2. Physiol Plant 139:256–268

Rao-Arelli AP (1994) Inheritance of resistance to *Heterodera glycines* race 3 in soybean accessions. Plant Dis 78:898–900

Riggs RD (1992) Chapter 10: host range. In: Riggs RD, Wrather JA (eds) Biology and management of the soybean cyst nematode. APS Press, St Paul, pp 107–114

Riggs RD, Hamblen ML (1962) Soybean-cyst nematode host studies in the Leguminosae. Ark Agric Exp Stn Rep Series 110 Fayetteville AR, p 17

Riggs RD, Hamblen ML (1966a) Additional weed hosts of *Heterodera glycines*. Plant Dis Rep 50:15–16

Riggs RD, Hamblen ML (1966b) Further studies on the host range of the soybean-cyst nematode. Ark Agric Exp Stn Bulletin 718 Fayetteville AR, p 19

Riggs RD, Kim KS, Gipson I (1973) Ultrastructural changes in Peking soybeans infected with *Heterodera glycines*. Phytopathology 63:76–84

Rodriguez-Saona C, Maynard DF, Phillips S, Trumble JT (2000) Avocadofurans and their tetrahydrofuran analogues: comparison of growth inhibitory and insecticidal activity. J Agric Food Chem 48:3642–3645

Ross JP (1958) Host-Parasite relationship of the soybean cyst nematode in resistant soybean roots. Phytopathology 48:578–579

Ross JP, Brim CA (1957) Resistance of soybeans to the soybean cyst nematode as determined by a double-row method. Plant Dis Rep 41:923–924

Savchenko T, Walley JW, Chehab EW, Xiao Y, Kaspi R, Pye MF, Mohamed ME, Lazarus CM, Bostock RM, Dehesh K (2010) Arachidonic acid: an evolutionarily conserved signaling molecule modulates plant stress signaling networks. Plant Cell 22:3193–3205

Scheideler M, Schlaich NL, Fellenberg K, Beissbarth T, Hauser NC, Vingron M, Slusarenko AJ, Hoheisel JD (2002) Monitoring the switch from housekeeping to pathogen defense metabolism in *Arabidopsis thaliana* using cDNA arrays. J Biol Chem 277:10555–105561

Schmelzer E (2002) Cell polarization, a crucial process in fungal defence. Trends Plant Sci 7:411–415

Schmutz J, Cannon SB, Schlueter J, Ma J, Mitros T, Nelson W, Hyten DL, Song Q, Thelen JJ, Cheng J, Xu D, Hellsten U, May GD, Yu Y, Sakurai T, Umezawa T, Bhattacharyya MK, Sandhu D, Valliyodan B, Lindquist E, Peto M, Grant D, Shu S, Goodstein D, Barry K, Futrell-Griggs M, Abernathy B, Du J, Tian Z, Zhu L, Gill N, Joshi T, Libault M, Sethuraman A, Zhang XC, Shinozaki K, Nguyen HT, Wing RA, Cregan P, Specht J, Grimwood J,

Rokhsar D, Stacey G, Shoemaker RC, Jackson SA (2010) Genome sequence of the palaeopolyploid soybean. Nature 463:178–183

Shannon JG, Arelli PR, Young LD (2004) Breeding for resistance and tolerance. In: Schmitt DP, Wrather JA, Riggs RD (eds) Biology and management of soybean cyst nematode, 2nd edn. Schmitt & Associates of Marceline, Marceline, pp 155–180

Shen B, Li C, Tarczynski MC (2002) High free-methionine and decreased lignin content result from a mutation in the Arabidopsis S-adenosyl-L-methionine synthetase 3 gene. Plant J 29:371–380

Smigocki A, Neal JW Jr, McCanna I, Douglass L (1993) Cytokinin-mediated insect resistance in Nicotiana plants transformed with the ipt gene. Plant Mol Biol 23:325–335

Steppuhn A, Gase K, Krock B, Halitschke R, Baldwin IT (2004) Nicotine's defensive function in nature. PLoS Biol 2:E217

Tang F, Lao K, Surani MA (2011) Development and applications of single-cell transcriptome analysis. Nat Methods 8:S6–S11

Veronese P, Nakagami H, Bluhm B, Abuqamar S, Chen X, Salmeron J, Dietrich RA, Hirt H, Mengiste T (2006) The membrane-anchored BOTRYTIS-INDUCED KINASE1 plays distinct roles in Arabidopsis resistance to necrotrophic and biotrophic pathogens. Plant Cell 18:257–273

Winstead WW, Skotland CB, Sasser JW (1955) Soybean cyst nematode in North Carolina. Plant Dis Rep 39:9–11

Wrather JA, Koenning SR (2006) Estimates of disease effects on soybean yields in the United States 2003–2005. J Nematol 38:173–180

Xia Y, Yu K, Navarre D, Seebold K, Kachroo A, Kachroo P (2010) The glabra1 mutation affects cuticle formation and plant responses to microbes. Plant Physiol 154:833–846

Zulak KG, Weljie AM, Vogel HJ, Facchini PJ (2008) Quantitative 1H NMR metabolomics reveals extensive metabolic reprogramming of primary and secondary metabolism in elicitor-treated opium poppy cell cultures. BMC Plant Biol 8:5